Wetlands Ecol Manage (2007) 15:51–62
DOI 10.1007/s11273-006-9011-9

ORIGINAL PAPER

Natural and anthropogenic changes to mangrove distributions in the Pioneer River Estuary (QLD, Australia)

Stacy D. Jupiter · Donald C. Potts · Stuart R. Phinn · Norman C. Duke

Received: 17 April 2006 / Accepted: 19 April 2006 / Published online: 7 October 2006

Abstract We analyzed a time series of aerial photographs and Landsat satellite imagery of the Pioneer River Estuary (near Mackay, Queensland, Australia) to document both natural and anthropogenic changes in the area of mangroves available to filter river runoff between 1948 and 2002. Over 54 years, there was a net loss of 137 ha (22%) of tidal mangroves during four successive periods that were characterized by different driving mechanisms: (1) little net change (1948–1962); (2) net gain from rapid mangrove expansion (1962–1972); (3) net loss from clearing and tidal isolation (1972–1991); and (4) net loss from a severe species-specific dieback affecting over 50% of remaining mangrove cover (1991–2002). Manual digitization of aerial photographs was accurate for mapping changes in the boundaries of mangrove distributions, but this technique underestimated the total loss due to dieback. Regions of mangrove dieback were identified and mapped more accurately and efficiently after applying the Normalized Difference Vegetation Index (NDVI) to Landsat Thematic Mapper satellite imagery, and then monitoring changes to the index over time. These remote sensing techniques to map and monitor mangrove changes are important for identifying habitat degradation, both spatially and temporally, in order to prioritize restoration for management of estuarine and adjacent marine ecosystems.

Keywords Aerial photography · Dieback · Land use · Mangroves · Landsat · Australia · Queensland · Pioneer River Estuary

S. D. Jupiter (✉) · D. C. Potts
Department of Ecology and Evolutionary Biology, A316 Earth and Marine Sciences, University of California, 1156 High Street, Santa Cruz, CA 95064, USA
e-mail: jupiter@biology.ucsc.edu

S. R. Phinn · S. D. Jupiter
Centre for Remote Sensing and Spatial Information Science, School of Geography, Planning & Architecture, University of Queensland, St. Lucia, 4072 QLD, Australia

N. C. Duke · S. D. Jupiter
Centre for Marine Studies, University of Queensland, St. Lucia, 4072 QLD, Australia

Introduction

Globally, about one third of mangrove forests have been lost within the past 50 years (Alongi 2002). This has resulted in growing concern over the coincident decline of important mangrove ecosystem services, such as filtering runoff and providing fisheries habitat, which are critical for maintaining ecological integrity in downstream ecosystems. While mangroves and tidal flats comprise only a small portion of catchment area, they trap and store disproportionate amounts of suspended particles, nutrient-rich organic matter, and associated pollutants from catchment runoff (Woodroffe 1992; Tam and Wong 1995; Furukawa and Wolanski 1996; Victor et al. 2004; Alongi and McKinnon 2005; Alongi et al. 2005). Mangroves are also connected to adjacent ecosystems through fishery links. For example, mangrove habitat boosts adult fish and invertebrate biomass on adjacent reefs by providing a refuge for juveniles of species that exhibit ontogenetic shifts (Nagelkerken et al. 2000; Mumby et al. 2004), and fishery catch per unit effort data from Queensland, Australia, has been significantly correlated to mangrove area and perimeter for mangrove-related species (Manson et al. 2005). In order to assess potential impacts of recent mangrove loss on downstream ecosystems, it is first necessary to quantify the magnitude of anthropogenic change relative to natural changes as certain types of change are more likely to permanently alter mangrove ecosystem condition and therefore affect its ecosystem services.

With synoptic, non-intrusive data collection over large areas, remote sensing offers distinct advantages for quantifying vegetation changes over time and for examining the biophysical properties of mangroves in regions where fieldwork is difficult (Green et al. 1996, 1997). Aerial photography has been used not only to map broadscale mangrove distributions (Saintilan and Wilton 2001), but also to classify dominant species and assemblages (Sulong et al. 2002; Verheyden et al. 2002), evaluate tree density (Verheyden et al. 2002), and then to monitor these parameters over time (Dahdouh-Guebas et al. 2000, 2004; Lucas et al. 2002). Despite recent advances in sensor technology, the labor intensity required for digitization, and the subjectivity of photo-interpretation, aerial photography remains a preferred platform for mapping mangrove distributions, particularly in developing countries (Dahdouh-Guebas 2002).

Data from multispectral satellite sensors such as SPOT (Système Pour l'Observation de la Terre) and Landsat Thematic Mapper (TM) and Enhanced Thematic Mapper (ETM) are also useful for discriminating mangrove from non-mangrove zones (Rasolofoharinoro et al. 1998; Gao 1999; Blasco and Aizpuru 2002; Haito et al. 2003) and are often more cost-effective than aerial photographs due to high processing efficiency (Mumby et al. 1999). In addition, multi-band spectral data, unlike traditional aerial photographs, can be used to calculate vegetation indices based on differences in reflectance properties of vegetation in different wavelengths, typically between the red and near-infrared (NIR) wavelengths. These differences have been correlated with biophysical properties of the mangrove canopy; for example, mangrove Normalized Difference Vegetation Index (NDVI) values have been correlated with biomass, canopy cover and Leaf Area Index (LAI) (Jensen et al. 1991; Ramsey and Jensen 1996; Green et al. 1997, 1998; Green and Mumby 2000).

We quantify mangrove loss in the Pioneer River Estuary and identify drivers of mangrove distribution changes at decadal intervals (spanning 54 years; 1948–2002) from aerial photographs in order to assess the magnitude of anthropogenic versus natural change. We specifically focus on documenting changes to mangrove areas that are hydrologically connected to the Pioneer River flow and therefore potentially act as sinks for material contained in catchment runoff. Mangroves in the Pioneer Estuary, near Mackay on the central Queensland coast, were especially appropriate for this study because the estuary: (1) has a long history of anthropogenic modification (beginning in 1887 with the construction of training walls to stabilize the river channel) (Gourlay and Hacker 1986); and (2) has recently experienced high mortality (dieback) of trees, with the dominant and normally broadly tolerant mangrove, *Avicennia marina* (Forssk.) Vierh., being the most obviously affected species (Duke et al. 2005). We additionally investigate the application of the NDVI from Landsat TM and ETM imagery to map and monitor the spatial and temporal progression of canopy loss associated with tree death throughout the Pioneer Estuary. Change detection analysis using NDVI calculated from satellite data is applied routinely in forest and agricultural management (Washmon et al. 2002; Wilson and Sader 2002), and change detection has been used successfully with visual interpretation techniques to track mangrove

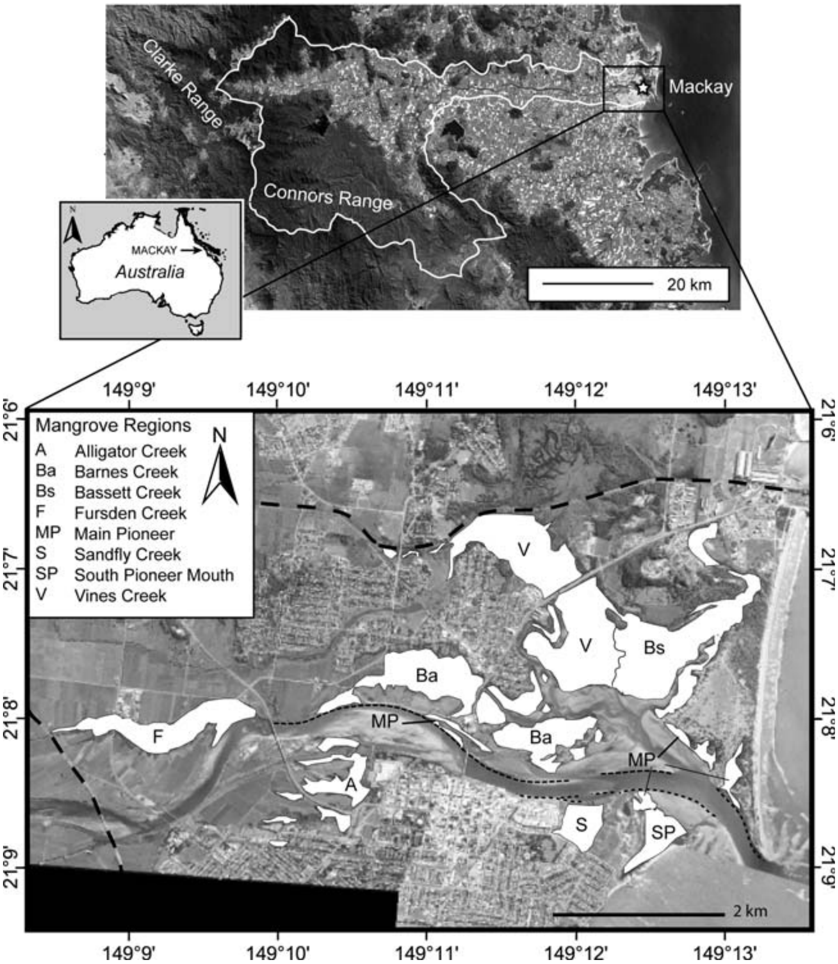

Fig. 1 Above: Mackay (star) and the Pioneer catchment (white outline) on a Landsat 7 ETM image, captured 16 July 2000. Dark areas indicate remnant natural vegetation; light areas indicate development and land cleared for sugarcane cultivation. The Pioneer Estuary lies within the black box. Below: Eight mangrove sub-regions (white) within the Pioneer Estuary. Major urban features include a railway (thick dashed line) and training walls (thin dashed line) along the north and south banks of the Pioneer River

dieback in the Ganges Delta (Blasco et al. 2001) and in French Guiana (Fromard et al. 2004).

Methods

Regional and local setting

The Pioneer catchment (Fig. 1; 21°–21°25′ S; 148°30′–149°15′ E) covers 1570 km^2 (GBRMPA 2001). Upper catchment soils are derived largely from granites and granodiorites of the igneous Urannah complex, forming the Clarke and Connors ranges to the W and SW (Gourlay and Hacker 1986). Lower catchment soils are dominated by Quaternary alluvium on the flood plain of the Pioneer River, which stretches 75 km from the ranges to the sea (Gourlay and Hacker 1986). The climate is characterized by high seasonal rainfall, mainly during the summer cyclone season (December–April), with cyclone driven flooding occurring every 14–16 years (Marion et al. 2006). Mean annual rainfall (1586 mm ± 543 mm SD[1]) and, therefore mean annual discharge (0.808 km^3 ± .726 km^3 SD[2]), varies considerably between years, influenced by the monsoon trough and regional ENSO oscillations (Hacker 1988).

Sugarcane cultivation began in the Pioneer catchment in 1865 and expanded rapidly (Gourlay and Hacker, 1986). The catchment currently has the second highest proportion of cropped land (19%) among all GBR catchments, while 74% of catchment land is grazed and only 7% remains

[1] Digital data supplied by Australian Bureau of Meteorology, 1916–2003.

[2] Digital data supplied by Queensland Department of Natural Resources and Mines, 1916–2003.

under relatively natural conditions (Rayment and Neil 1997; GBRMPA 2001). The high percentage of cropped lands, combined with the soil composition and steep topography of the drainage, all contribute to one of the highest rates (per unit area) of sediment export from any GBR catchment (Moss et al. 1992). Two dams and three major weirs across the Pioneer River and its tributaries retain a high percentage of coarse sediments from the upper catchment (QDNRM 2001), but most fine sediment flows downstream to be deposited in and around the Pioneer Estuary (Gourlay and Hacker 1986).

There are at least 17 different mangroves species present within the Pioneer Estuary, with communities dominated by *Avicennia marina*, *Rhizophora stylosa* and *Ceriops australis* (Finglas et al. 1995; Duke et al. 2001). Local citizens first expressed concerns about tree death in the Pioneer Estuary in the early 1990's when dieback became obvious, predominantly affecting the grey mangrove, *A. marina*, known for its broad tolerances along latitudinal and salinity gradients and high resilience to physical damage (Tomlinson 1986; Duke 1991; Duke et al. 1998). As of 2002, moderate to severe dieback of *A. marina* affected 58% of mangrove area in the region, including the Pioneer Estuary (Duke et al. 2005). Preliminary observations suggest that erosion and bank destabilization in tidal creeks has accelerated in dieback regions (Duke et al. 2005), amplified by strong currents from up to 6.5 m tides.

Mapping mangrove change through time

Black and white (1948, 1962, 1972, 1982, 1991) and color (1998, 2002) aerial photographs covering the Pioneer Estuary and the city of Mackay (Fig. 1), at scales of 1:10,000–1:30,000, were borrowed from Queensland Department of Natural Resources and Mines and the Marine Botany Group at the University of Queensland. Individual photographs were scanned at 600 dpi and mosaicked using Adobe Photoshop Elements 2.0. The 1998 mosaic was georeferenced to part of an orthorectified Landsat ETM map product image captured on 16 July 2000 using ENVI 3.6 software. All other mosaics were georeferenced to the 1998 mosaic. Output pixel resolution for each mosaic was standardized to 1.2×1.2 m. Mangrove distributions (to nearest ha) within the delineated region of the Pioneer River Estuary were manually digitized (for each year except 1998) based on tone, texture, contrast with adjacent substrates, and field knowledge using ArcView 3.2 software. Mangrove regions cut off from main tidal flow as a result of hydrological modifications to the estuary were categorized as non-tidal. These regions are reported, but unlike new mangrove area, they were not included in the overall total of mangrove area available for filtering catchment runoff. Probable drivers of change, based on definitions in Schaffelke et al. (2005), were identified after visually comparing successive maps.

Normalized Difference Vegetation Index

The Pioneer Estuary subset of the 2000 Landsat ETM image (16 July 2000) was radiometrically matched to a 1990 Landsat TM image (24 April 1990) using an empirical line calibration to correct for differences in solar irradiance and atmospheric path radiance (Yuan et al. 1998). A mask exposing only the mangrove areas within the Pioneer Estuary was created by digitizing the 1990 Landsat TM image and then used to define the estuary area in the corrected 2000 Landsat ETM image. NDVI images for the identical areas in 1990 and 2000 Landsat images were then produced. The unitless NDVI (ranging from –1 to +1) was calculated as: NDVI = (NIR – Red)/(NIR + Red), where NIR is the % reflectance in the near infrared (Landsat Band 4; 0.76–0.90 μm) and Red is the % reflectance in the visible red (Landsat Band 3; 0.63–0.69 μm) (Rouse et al. 1974).

To determine whether NDVI is an acceptable proxy measure of dieback in the Pioneer Estuary, the variance of the 2000 Landsat ETM image NDVI values (dependent variable) was partitioned between field measures of live mangrove density and basal area of dead trees (independent variables) in a multiple regression analysis (Sokal and Rohlf 1995). Both dead basal area and live tree density are functions of the intensity and extent of mangrove dieback in the Pioneer Estuary. Field data were collected between May 2003 and March 2004 in 5 m $\times$ 5 m plots. Species, stem circumference and health status (alive/dead) were recorded for all trees ≥1 m in high.

To evaluate changes within the estuary between 1990 and 2000, a difference image was calculated from the 1990 and 2000 NDVI images: for each pixel, $D = (\mathrm{NDVI}_{1990} + 1) - (\mathrm{NDVI}_{2000} + 1)$, with 1 added to all NDVI values to avoid the subtraction of negative values. The change for each pixel in the difference image was classified as ''NDVI lower'' ($D < -0.05$), ''no change'' ($D = -0.05$–0.30) or ''NDVI higher'' ($D > 0.30$). Correlations between NDVI change classes and changes in mangrove canopy density were assessed in a normalized 2×2 error matrix (Congalton 1991). Georeferenced aerial photographs from 1991 and 1998, the two closest dates for which aerial photographs were available within the bounds (1990–2000) of the change detection analysis, served as reference images. One hundred and fifty points were selected for comparisons using a stratified random sampling design. Paired points (1991, 1998) on the aerial photographs were visually assessed for increases or decreases in mangrove canopy density and compared against the calculated NDVI class. The ''no change'' class was not included in the overall matrix because we were unable to reliably determine if the corresponding paired points visually showed no change in canopy density. The error matrix summarizes the overall correlation between the NDVI map and reference data, as well as the ''user's'' and ''producer's'' accuracies: user's accuracy is the probability that a classified NDVI pixel correctly represents the mangrove density change (observed in aerial photographs); producer's accuracy is the probability that a pixel (in any class) has been correctly classified (Congalton 1991).

Results

Mangrove distribution changes, 1948–2002

From 1948 to 2002, the total area of mangroves available to filter river runoff within the delineated region of the Pioneer Estuary decreased from 634 to 497 ha (by 22%), principally from such anthropogenic activities as clearing, filling and altering the natural hydrodynamic structure of the estuary. The proportions of mangrove changes attributed to clearing/natural loss, tidal isolation from hydrological manipulations and new growth are summarized in Table 1. Mangroves were cleared at an average rate of ~4 ha/yr for both agricultural and urban expansion, although large-scale changes were typically episodic in frequency. New highways, levees and a railway line isolated persistent patches of mangroves that were treated as permanent exclusions from the total hectares available for filtration of runoff. The total loss of mangroves (274 ha) within this region was partially offset by 137 ha of new growth (Table 1), which occurred predominantly in Barnes Creek and at river bends (by Fursden Creek, the southwest bank of Bassett Basin, and the south bank near the Pioneer River mouth), where decreased velocity facilitated recent sediment deposition.

Distribution change from mangrove dieback

Mangrove dieback was quantifiable only in the 2002 aerial photomosaic, where it appears as small canopy gaps, either as light brown areas of visible muddy substrate or as dark patches caused by tree shadows. Due to the labor and time required

Table 1 Changes in mangrove areas (to nearest ha) mapped from aerial photographs between 1948 and 2002. Values for non-tidal, cleared or lost, and new growth areas are reported relative to the previous time interval

Year	Total	Change			Net change (ha)
	Tidally flushed (ha)	Non-tidal (ha)	Cleared/Lost (ha)	New growth (ha)	
1948	634				
1962	625	0	66	57	–9
1972	658	5	25	63	+33
1982	567	35	66	10	–91
1991	522	3	44	2	–45
2002	497	10	20	5	–25
Net change	–137	–53	–221	+137	–137

to accurately digitize every gap, estuary-scale mapping of mangrove distribution from visual interpretation of aerial photographs underestimated the magnitude of mangrove loss. Fortunately, mangrove dieback can be mapped much more quickly (hours vs. weeks) from satellite imagery. The NDVI analysis applied to Landsat satellite images integrated proportions of different surfaces (e.g. bare ground, thin canopy, thick canopy) within each 28.5 m × 28.5 m image pixel. Pixels with exposed mud, thinner canopies and/or large proportions of defoliated, dead trees (more dieback) had lower NDVI values than pixels with only dense mangrove canopy.

In a multiple regression analysis of NDVI values and tree characteristics measured in the field, the relationship between NDVI and dead basal area was significant (Fig. 2a; $p = 0.047$), but the relationship between NDVI and live mangrove density was not significant ($p = 0.553$). However, the latter result is probably biased by the 3 year temporal lag between the 2000 Landsat ETM image and the collection of field data: the NDVI values from the easternmost Bassett Creek site were higher than expected because, by 2003–04, severe dieback had spread from west to east across the estuary, thinning canopies and opening gaps as *Avicennia marina* died and became uprooted. When pixels from Bassett Creek were excluded from the analysis, the correlation between NDVI and live tree density was significant ($r = 0.738$, $P < 0.01$, $n = 12$) (Fig. 2b).

In the alternative approach to mapping dieback using change detection of the 1990 and 2000 NDVI images, 44 ha (543 pixels) were classified as lower NDVI in 2000, and 56 ha (687 pixels) were classified as higher NDVI (Fig. 3). Dieback was most pronounced around creek margins, where *A. marina* trees are both numerous and large. In the error analysis, the overall accuracy (98%) indicates a very strong association between NDVI change calculated from Landsat images and canopy density changes from aerial photographs (Table 2).

Discussion

Drivers of mangrove change in the Pioneer Estuary

In the past few decades, there has been a surge of studies documenting changes in global mangrove distributions (Spalding et al. 1997). Certain changes are directly anthropogenic in origin and result in both gains (e.g. large-scale mangrove afforestation in Bangladesh; Saenger and Siddiqi 1993) and losses (e.g. mangrove conversion to shrimp aquaculture in SE Asia; Spalding et al. 1997; Tong et al. 2004). Other changes, such as hydrological alterations, manifest as indirect effects of human activity: for example, the top-dying of *Heritiera fomes* in the Ganges Delta is likely to be a result of construction of embankments

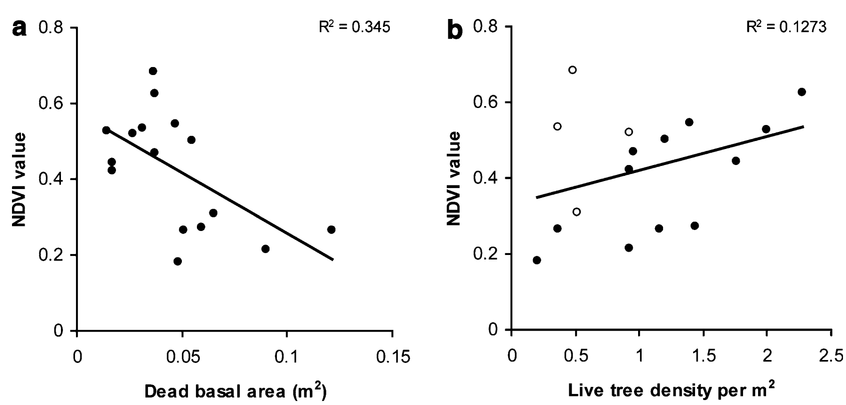

Fig. 2 NDVI values derived from 2000 Landsat ETM data plotted against *in situ* measurements of: (**a**) dead basal area (m^2); and (**b**) live tree density per m^2. Closed circles are sites from Fursden, Barnes and Vines Creeks; open circles are sites from Bassett Creek

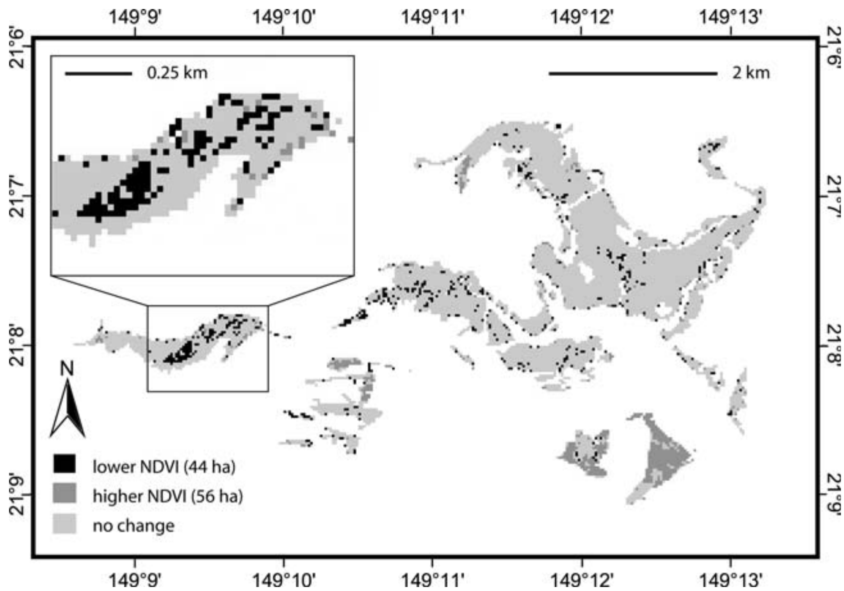

Fig. 3 Differences in NDVI values between 1990 and 2000. Light grey regions indicate areas of no change. The high densities of black pixels in Fursden Creek (inset) indicate areas of heavy dieback

and dams upstream to mangrove regions (Spalding et al. 1997). Other changes result from distinctly natural processes, such as extensive mangrove loss in the Lesser Antilles from hurricane damage (Imbert et al. 1996; Imbert et al. 2000) or rapid losses/gains from cycles of erosion and accretion at the Amazon River delta (Fromard et al. 2004). Because some types of change are more likely to destabilize mangrove ecosystems and impact mangrove ecosystem services (e.g. sediment trapping, availability of fisheries habitat), it is important to determine the magnitudes of each type of disturbance and the projected rates of recovery before we can assess potential impacts to adjacent ecosystems (e.g. seagrass beds, coral reefs).

Different, dominant processes can be ascribed to four distinct periods of change in the distributions of Pioneer Estuary mangroves in the past sixty years (Fig. 4). During the first period (1948–1962), large-scale clearing in Alligator Creek (in response to an extreme flood in 1958) and Bassett Creek (for harbor expansion) was effectively matched by rapid mangrove expansion to yield little net change. Two mechanisms drove mangrove expansion during this period: wetter climate and newly deposited substrate on which to colonize. Natural rates of mangrove expansion and contraction are highly sensitive to climatic variation. For example, the proportion of mangroves relative to saltpans in unaltered estuaries can be reliably predicted from the mean annual rainfall alone (Fosberg 1961; Bucher and Saenger 1994). Indeed, the rapid growth of mangroves during the 1950's in Barnes Creek corresponded with a period of increased rainfall that may have

Table 2 Error matrix for associations between NDVI change classes (1990–2000) and canopy density changes (1991–1998). Data are the numbers (out of 150) of 28.5 × 28.5 m (Landsat-sized) pixels cross-classified between the NDVI difference image and the difference between 1991 and 1998 aerial photomosaics

		Canopy density change (1991–1998) (Aerial photographs)		User's accuracy
		Density decreased	Density increased	
NDVI difference (1990–2000)	NDVI lower	59	1	98.3%
(Satellite data)	NDVI higher	2	88	97.8%
Producer's accuracy		96.7%	98.9%	**98.0%**

The overall correlation accuracy is in bold text. The ''no change'' class was excluded from analysis

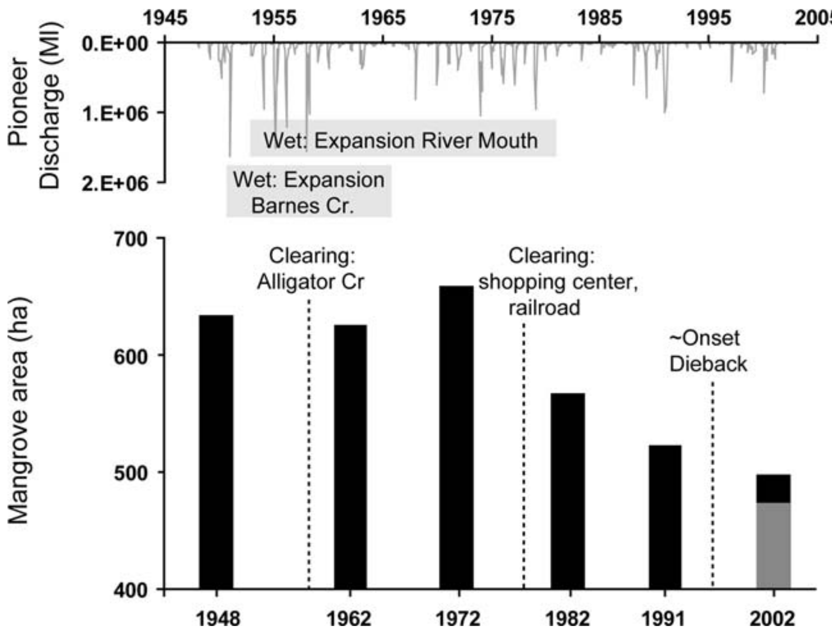

Fig. 4 Time series of changes in Pioneer Estuary mangrove area (below) plotted with Pioneer River discharge (above). Black bars represent the total tidal mangrove area digitized from aerial photography. The vertical grey bar represents the 2002 mangrove area adjusted for the additional amount of mangrove loss mapped from change detection of NDVI from Landsat satellite data. Dashed lines denote approximate timing of major mangrove losses. Horizontal grey bars cover periods of major mangrove expansion

reduced salinity and facilitated colonization (Gourlay and Hacker 1986) (Fig. 4). Similarly, just as rainfall enabled mangrove colonization onto previously uninhabitable substrate, new deposits of fine muds and silts along river bends following major floods facilitated rapid mangrove settlement of pioneer species onto previously unavailable substrate, particularly along the south bank of the Pioneer River mouth where mangroves expanded northeastward from Town Beach.

During the second period (1962–1972), mangrove expansion outpaced clearing activities; mangroves expanded in Barnes Creek, where established trees probably provided shade and encouraged new growth by limiting evaporation (Gourlay and Hacker 1986), and along newly deposited sediments along river bends. Mangroves also recolonized some previously cleared areas, such as along Alligator Creek. While these new mangroves may have provided additional filtration of catchment runoff and new fisheries habitat, the accelerated rate of mangrove expansion may itself be symptomatic of changes in upstream land use. Rapid mangrove expansion is indicative of a number of factors, including processes leading to increased sediment and nutrient concentrations in estuarine waters (Gourlay and Hacker 1986; Duke and Wolanski 2001). Thus, the new growth in the Pioneer Estuary may be a response to the estimated two to four-fold increase in sediment delivery to the estuary since initial land clearing (Hacker 1988).

Mangrove expansion decelerated through the third period (1972–1991), which was characterized instead by large-scale infilling of the estuary, preventing any future recovery of mangroves within these regions. There was little new expansion to replace losses from the major development activities of the late 1970s and 1980s (e.g. railway, shopping center, port expansion) that claimed 110 ha of mangroves and isolated another 38 ha from regular tidal flushing. This mangrove loss substantially reduced (by 22%) the mangrove area available to function as sediment and nutrient sinks and to provide refuge habitat for juvenile fish.

The fourth period of mangrove change (1991–2002) was dominated by the onset of the mangrove dieback. Although the proportion of mangroves lost during this period is less than in 1972–1991, the consequences of dieback may be magnified in severity by the location of large *Avicennia marina* trees mainly along creek margins and tidal banks: within large gaps, previously deposited sediments are remobilized and actively eroded. Exposed cable roots of *A. marina* trees suggest that sediments eroded following decomposition of live fibrous roots, which may lose 30–52% of original mass after 154 days following death (Albright 1976). Although there is clear visual evidence of bank destabilization in regions of severe dieback and sediment loss associated with uprooted trees, the fate of this material and its contribution to nearshore water quality has not yet been quantified.

Assessment of techniques for mapping mangrove dieback

The value of aerial surveys for studies of mangrove ecosystems has long been recognized, given the impenetrability of many forests, but while aerial photographs effectively capture detailed changes in mangrove distributions, they have several disadvantages (e.g. misregistration problems, high processing time, low spectral sampling) compared with newer satellite and airborne sensors for mapping natural and anthropogenic changes within the canopy. The accuracy of land cover change maps is determined by the relative geometric accuracy of the remotely sensed datasets (Townshend et al. 1992; Phinn and Rowland 2001). Thus, unless data are available to orthorectify historical aerial photographs, any change detection analyses using these sources may encounter substantial misregistration between sets of photographs, which becomes pronounced at ecotone boundaries. Misregistration errors are minimal for satellite sensors, particularly those with sun-synchronous orbits, such as Landsat or SPOT, that pass over target locations at regular intervals, at the same time of day, and with the same look angle. The 2000 Landsat ETM image selected for this study had a root mean square error (RMSE) of 0.25 pixels (pixel size = 28.5 m × 28.5 m; n = 20) relative to the 1990 Landsat TM image, which is within the acceptable limits for geometric accuracy (0.5–1.0 pixels) recommended for change detection analyses (Jensen 2000; Phinn and Rowland 2001). By contrast, RMSE's for the aerial photomosaics ranged between 14.5 and 40.6 pixels (pixel size = 1.2 m × 1.2 m; n = 20), prohibiting change detection of mangrove classifications between successive datasets.

The maps from aerial photography in this study underestimated the amount of mangrove loss from dieback because of both the patchiness of affected trees and the large time and labor commitments for digitizing small canopy gaps. A more efficient and accurate method of dieback mapping is to use the NDVI index applied to satellite imagery. The significant correlations of NDVI with dead basal area and live tree density (after excluding Bassett sites), plus the 98% correspondence with observed changes in canopy cover (from aerial photography) between 1990 and 2000, indicate that NDVI is an acceptable proxy for dieback in this region, though its application may not be universal. Despite a significant relationship with NDVI, dead basal area only explains 28% of the variation in NDVI values. The high unexplained variation could be attributed to many factors, including the low sample size, the discrepancy in size between field plots (5 m × 5 m) and Landsat pixels (28.5 m × 28.5 m), and the lag time between image acquisition and field data collection, which particularly affected the plots in Bassett Creek. The low correlation between NDVI and live tree density (before exclusion of Bassett sites) would probably increase if data were weighted by size of trees: the model used assumes equal sizes for all trees measured, even though larger trees have higher leaf production (Coulter et al. 2001) and therefore exert proportionally greater influence on NDVI values than smaller trees.

Using airborne or satellite sensors with higher spatial resolutions and spectral sampling intervals (e.g. IKONOS, Quickbird, IRS, SPOT 5, HyMap) should also strengthen correlations between NDVI and mangrove dieback. For example, mangrove mapping in the Turks and Caicos Islands using the multispectral Compact Airborne Spectographic Instrument (CASI) (1 m × 1 m pixel; 8 user-defined bands) improved the accuracy of a regression model converting NDVI to leaf area index (within a 95% confidence interval) from 88% with the SPOT XS satellite (20 m × 20 m pixel; 3 bands) (Green et al. 1997) to 94% (Green et al. 1998). The improved spatial resolution of the CASI sensor, as well as the choice of spectral bands, also enabled mangrove classifications based on height, density and dominant species with reasonable accuracy (78% for six mangrove classes; 86% for four classes) (Green et al. 1998). Similar results have also been achieved with very high spatial resolution multispectral data (e.g. IKONOS, Quickbird; Wang et al. 2004) and high spatial resolution hyperspectral data integrated with radar (e.g. CASI and AIRSAR; Held et al. 2003), each of which offers advantages in high diversity mangrove ecosystems. Radar has proven valuable for discrimination of degraded mangroves (open canopy) from intact forest (closed canopy) based on increased backscatter from C-, L- and P-band frequencies (Proisy et al. 2002), and its integration with optical data should improve dieback classifications.

Conclusions

Mangrove area in the Pioneer River Estuary fluctuated between 1948 and 2002 in response to both natural and anthropogenic drivers of change, with proportionally greater impacts in recent decades from human activities. Certain changes, such as direct damage through wetland infilling for urban and agricultural encroachment, prevent recolonization and therefore result in a permanent loss of mangrove area available for filtering runoff and providing fish habitat. These changes can be identified using remote sensing tools, which are additionally valuable for identifying regions of degraded habitat and prioritizing sites for restoration in order to maintain the ecosystem functions and services that ultimately preserve biogeochemical and ecological links between mangroves and their adjacent marine habitats.

Acknowledgements Funding for this work was provided by a Postgraduate Fulbright Fellowship, a NASA Graduate Student Researchers Programs Fellowship and a PADI Foundation award. We thank Greg Tooth, Judith Wake and members of the Mackay Conservation Group for field assistance, Maureen Cooper of Padaminka Nature Refuge for providing accommodation and support, and Noel Whitehead of Sunfish Mackay for raising awareness of the mangrove dieback. We are grateful to Karen Joyce for data processing assistance.

References

Albright LJ (1976) *In situ* degradation of mangrove tissues. New Zeal J Mar Freshw Res 10:385–389

Alongi DM (2002) Present state and future of the world's mangrove forests. Environ Conserv 29:331–349

Alongi DM, McKinnon AD (2005) The cycling and fate of terrestrially-derived sediments and nutrients in the coastal zone of the Great Barrier Reef shelf. Mar Pollut Bull 51:239–252

Alongi DM, Pfitzner J, Trott LA, Tirendi F, Dixon P, Klumpp DW (2005) Rapid sediment accumulation and microbial mineralization in forests of the mangrove *Kandelia candel* in the Jiulongjiang Estuary, China. Estuar Coast Shelf Sci 63:605–618

Blasco F, Aizpuru M (2002) Mangroves along the coastal stretch of the Bay of Bengal: Present status. Indian J Mar Sci 31:9–20

Blasco F, Aizpuru M, Gers C (2001) Depletion of the mangroves of Continental Asia. Wetl Ecol Manage 9:245–256

Bucher D, Saenger P (1994) A classification of tropical and subtropical Australian estuaries. Aquat Conserv: Mar Freshw Ecosyst 4:1–19

Congalton R (1991) A review of assessing the accuracy of remotely sensed data. Remote Sens Environ 37:35–46

Coulter SC, Duarte CM, Tuan MS, Tri NH, Ha HT, Giang LH, Hong PN (2001) Retrospective estimates of net leaf production in *Kandelia candel* mangrove forests. Mar Ecol Progr Ser 221:117–124

Dahdouh-Guebas F (2002) The sustainable management of tropical coastal ecosystems. Environ Develop Sustain 4:93–112

Dahdouh-Guebas F, Verheyden A, De Genst W, Hettiarachchi S, Koedam N (2000) Four decadal vegetation dynamics in Sri Lankan mangroves as detected from sequential aerial photography: a case study in Galle. Bull Mar Sci 67:741–759

Dahdouh-Guebas F, Van Pottelbergh I, Kairo JG, Cannicci S, Koedam N (2004) Human-impacted mangroves in Gazi (Kenya): predicting future vegetation based on retrospective remote sensing, social surveys, and tree distribution. Mar Ecol Progr Ser 272:77–92

Duke NC (1991) A systematic revision of the mangrove genus *Avicennia* (Avicenniaceae) in Australasia. Aust Systemat Bot 4:299–324

Duke NC, Wolanski E (2001) Muddy coastal waters and depleted mangrove coastlines—depleted seagrass and coral reefs. In: Wolanski E (ed) Oceanographic processes of coral reefs: physical and biological links in the Great Barrier Reef. CRC Press, Boca Raton, Florida, USA, pp 77–91

Duke NC, Ball MC, Ellison JC (1998) Factors influencing biodiversity and distributional gradients in mangroves. Global Ecol Biogeogr Lett 7:27–47

Duke NC, Roelfsema CM, Tracey D, Godson LM (2001) Preliminary investigation into dieback of mangroves in the Mackay region. Marine Botany Group, The University of Queensland, Brisbane, Australia

Duke NC, Bell AM, Pederson DK, Roelfsema CM, Bengston-Nash S (2005) Herbicides implicated as the cause of severe mangrove dieback in the Mackay region, NE Australia: consequences for marine plant habitats of the GBR World Heritage Area. Mar Pollut Bull 51:308–324

Finglas AP, Winter D, Wild A (1995) Current distribution and historical comparisons of intertidal vegetation communties and saltpans in the Mackay region (Shoal Point to Hay Point). Queensland Department of Primary Industries

Fosberg FR (1961) Vegetation-free zone on dry mangrove coastline. US Geol Soc Profess Papers 424:216–218

Fromard F, Vega C, Proisy C (2004) Half a century of dynamic coastal change affecting mangrove shorelines of French Guiana. A case study based on remote sensing data analyses and field surveys. Mar Geol 208:265–280

Furukawa K, Wolanski E (1996) Sedimentation in mangrove forests. Mangroves and Salt Marshes 1:3–10

Gao J (1999) A comparative study on spatial and spectral resolutions of satellite data mapping in mangrove forests. Int J Remote Sens 20:2823–2833

GBRMPA (2001) Great Barrier Reef water quality: current issues. Great Barrier Reef Marine Park Authority, Townsville, Australia

Gourlay MR, Hacker JLF (1986) Pioneer River Estuary sedimentation studies. University of Queensland, Department of Civil Engineering, St. Lucia, Australia, 207 pp

Green E, Mumby P (2000) Mapping mangroves. In: Edwards AJ (ed) Remote sensing handbook for tropical coastal management. UNESCO, Paris, France, pp 183–198

Green EP, Mumby PJ, Edwards AJ, Clark CD (1996) A review of remote sensing for the assessment and management of tropical coastal resources. Coast Manage 24:1–40

Green EP, Mumby PJ, Edwards AJ, Clark CD, Ellis AC (1997) Estimating leaf area index of mangroves from satellite data. Aquat Bot 58:11–19

Green EP, Mumby PJ, Edwards AJ, Clark CD, Ellis AC (1998) The assessment of mangrove area using high resolution multispectral airborne imagery. J Coast Res 14:433–443

Hacker JLF (1988) Rapid accumulation of fluvially derived sands and gravels in a tropical macrotidal estuary: the Pioneer River at Mackay, North Queensland, Australia. Sediment Geol 57:299–315

Haito H, Bellan MF, Al-Habshi A, Aizpuru M, Blasco F (2003) Mangrove research and coastal ecosystem studies with SPOT-4 HRVIR and TERRA ASTER in the Arabian Gulf. Int J Remote Sens 24:4073–4092

Held A, Ticehurst C, Lymburner L, Williams N (2003) High resolution mapping of tropical mangrove ecosystems using hyperspectral and radar remote sensing. Int J Remote Sens 24:2739–2759

Imbert D, Labbe P, Rousteau A (1996) Hurricane damage and forest structure in Guadaloupe, French West Indies. J Trop Ecol 12:663–680

Imbert D, Rousteau A, Scherrer P (2000) Ecology of mangrove growth and recovery in the Lesser Antilles: state of knowledge and basis for restoration projects. Restor Ecol 8:230–236

Jensen JR (2000) Remote sensing of the environment: an earth resource perspective. Prentice Hall, Upper Saddle River, New Jersey, USA, 544 pp

Jensen JR, Ramsey E, Davis BA, Thoemke CW (1991) The measurement of mangrove characteristics in south-west Florida using SPOT multispectral data. Geocartogr Int 2:13–21

Lucas RM, Ellison JC, Mitchell A, Donelly B, Finlayson M, Milne AK (2002) Use of stereo aerial photography for quantifying changes in the extent and height of mangroves in tropical Australia. Wetl Ecol Manage 10:161–175

Manson FJ, Lonergan NR, Harch BD, Skilleter GA, Williams L (2005) A broad-scale analysis of links between coastal fisheries production and mangrove extent: a case-study for northeastern Australia. Fish Res 74:69–85

Marion GS, Hoegh-Guldberg O, McCulloch MT, Jupiter SD (2006) Coral isotopic records (δ^{15}N) of unprecedented land-use stress in Great Barrier Reef coastal communities. Eos Trans. AGU 87(36), Ocean Sciences Meeting Suppl., Abstract OS520-04

Moss AJ, Rayment GE, Reilly N, Best EK (1992) A preliminary assessment of sediment and nutrient exports from Queensland coastal catchments. Queensland Department of Primary Industries, Brisbane, Australia

Mumby PJ, Green EP, Edwards AJ, Clark CD (1999) The cost-effectiveness of remote sensing for tropical coastal resources assessment and management. J Environ Manage 55:157–166

Mumby PJ, Edwards AJ, Arias-González JE, Lindeman KC, Blackwell PG, Gall A, Gorczynska MI, Harborne AR, Pescod CL, Renken H, Wabnitz CCC, Llewellyn G (2004) Mangroves enhance the biomass of coral reef fish communities in the Caribbean. Nature 427:533–536

Nagelkerken I, van der Velde G, Gorissen MW, Meijer GJ, van't Hoff T, den Hartog C (2000) Importance of mangroves, seagrass beds and the shallow coral reefs as a nursery for important coral reef fishes, using a visual census technique. Estuar Coast Shelf Sci 51:31–44

Phinn SR, Rowland T (2001) Quantifying and visualizing geometric misregistration from Landsat Thematic Mapper imagery and its effects on change detection in a rapidly urbanizing catchment. Asian-Pacific Remote Sens GIS J 14:41–54

Proisy C, Mougin E, Fromard F, Trichon V, Karam MA (2002) On the influence of canopy structure on the radar backscattering of mangrove forests. Int J Remote Sens 23:4197–4210

QDNRM (2001) Pioneer Valley Water Resource Plan—Current environmental conditions and impacts of existing water resource development. Queensland Department of Natural Resources and Mines, Brisbane, Australia

Ramsey EW III, Jensen JR (1996) Remote sensing of mangrove wetlands: relating canopy spectra to site-specific data. Photogr Engineer Remote Sens 62:939–948

Rasolofoharinoro M, Blasco F, Bellan MF, Aizpuru M, Gauquelin T, Denis J (1998) A remote sensing based methodology for mangrove studies in Madagascar. Int J Remote Sens 19:1873–1886

Rayment GE, Neil DT (1997) Sources of material in river discharge. In: Proceedings of the The Great Barrier Reef: Science, Use and Management, Townsville, Australia, 42–58. Great Barrier Reef Marine Park Authority

Rouse IW, Haas RH, Schell IA, Deering DW (1974) Monitoring vegetation systems in the Great Plains with ERTS. In: Proceedings of the Third Earth Resources Technology Satellite-1 Symposium, 3010–3017

Saenger P, Siddiqi NA (1993) Land from the sea: the mangrove afforestation of Bangladesh. Ocean Coast Manage 20:23–39

Saintilan N, Wilton K (2001) Changes in the distribution of mangroves and saltmarshes in Jervis Bay, Australia. Wetl Ecol Manage 9:409–420

Schaffelke B, Mellors J, Duke NC (2005) Water quality in the Great Barrier Reef region: responses of mangrove, seagrass and macroalgal communities. Mar Pollut Bull 51:279–296

Sokal RR, Rohlf FJ (1995) Biometry: the principles and practice of statistics in biological research, 3rd edn. W. H. Freeman and Company, New York, USA, 887 pp

Spalding M, Blasco F, Field C (1997) World mangrove atlas. The International Society for Mangrove Ecosystems, Okinawa, Japan, 178 pp

Sulong I, Mohd-Lokman H, Mohd-Tarmizi K, Ismail A (2002) Mangrove mapping using Landsat imagery and aerial photographs: Kemaman district, Terengganu, Malaysia. Environ Develop Sustain 4:135–152

Tam NFY, Wong YS (1995) Mangrove soils as sinks for wastewater-borne pollutants. Hydrobiologia 295: 231–241

Tomlinson PB (1986) The botany of mangroves. Cambridge University Press, Cambridge, UK

Tong PHS, Auda Y, Populus J, Aizpuru M, Al-Habshi A, Blasco F (2004) Assessment from space of mangroves evolution in the Mekong Delta, in relation to extensive shrimp farming. Int J Remote Sens 25:4795–4182

Townshend JRG, Justice CO, Gurney C, McManus J (1992) The impact of misregistration on change detection. IEEE Trans Geosci Remote Sens 30:1054–1059

Verheyden A, Dahdouh-Guebas F, Thomaes K, De Genst W, Hettiarachchi S, Koedam N (2002) High-resolution vegetation data for mangrove research as obtained from aerial photography. Environ Develop Sustain 4:113–133

Victor S, Golbuu Y, Wolanski E, Richmond RH (2004) Fine sediment trapping in two mangrove-fringed estuaries exposed to contrasting land-use intensity, Palau, Micronesia. Wetl Ecol Manage 12:277–283

Wang L, Sousa WP, Gong P, Biging GS (2004) Comparison of IKONOS and Quickbird images for mapping mangrove species on the Caribbean coast of Panama. Remote Sens Environ 91:432–440

Washmon CN, Solie JB, Raun WR, Itenfisu DD (2002) Within field variability in wheat grain fields over nine years in Oklahoma. J Plant Nutr 25:2655–2662

Wilson EH, Sader SA (2002) Detection of forest harvest type using multiple dates of Landsat TM imagery. Remote Sens Environ 80:385–396

Woodroffe C (1992) Mangrove sediments and geomorphology. In: Robertson AI, Alongi DM (eds) Tropical mangrove ecosystems. American Geophysical Union, Washington D.C., USA, pp 7–36

Yuan D, Elvidge CD, Lunetta RS (1998) Survey of multispectral methods for land cover change analysis. In: Lunetta RS, Elvidge CD (eds) Remote sensing change detection: environmental monitoring methods and applications. Sleeping Bear Press, Inc., Chelsea, Michigan, USA, pp. 21–39